

Decay Free Microwave Magnetic Envelope Soliton Pulse Trains in Yttrium Iron Garnet Thin Films

Boris A. Kalinikos,* Nikolai G. Kovshikov,* and Carl E. Patton

Department of Physics, Colorado State University, Fort Collins, Colorado 80523

(Received 27 December 1996)

Microwave magnetic envelope soliton pulse trains with no decay in amplitude have been obtained in magnetic films for the first time. The solitons were formed from magnetostatic spin waves with negative dispersion, or backward volume waves, propagated in a long and narrow $5.2 \mu\text{m}$ thick yttrium iron garnet film strip biased at 1096 Oe. An interrupted feedback technique was used to produce the soliton pulse trains from an initial 25 ns wide input pulse at a carrier frequency of 5.0 GHz. The train extended for over $40 \mu\text{s}$, 2 orders of magnitude longer than the single soliton lifetime. Measurements of the soliton width and phase profiles confirmed the soliton nature of the pulses over the entire train. [S0031-9007(97)02877-9]

PACS numbers: 75.30.Ds, 76.50.+g, 85.70.Ge

In the last three decades, soliton excitations have been realized in many physical systems [1–4]. In recent years, the processes of formation, propagation, and collision of microwave magnetic envelope (MME) solitons have been observed in yttrium iron garnet (YIG) films with various surface spin pinning conditions and under different propagation conditions [5–11]. Dissipation plays a significant role in limiting the propagation of these MME solitons. As found experimentally and verified theoretically, even for high quality low loss YIG films, dissipation restricts the single soliton lifetime to a few hundred nanoseconds or so [11]. For both fundamental and practical reasons, it would be very desirable to compensate the effects of loss by some amplification or feedback mechanism and thereby obtain long lived MME solitons.

This Letter reports the first experimental demonstration of a decay free train of MME soliton pulses in a YIG film with a duration up to $40 \mu\text{s}$, much longer than the 100–500 ns soliton lifetime given above. These soliton trains were obtained from 5.0 GHz magnetostatic backward volume wave pulses propagated in a narrow YIG film strip. The formation of a stable train of soliton pulses without decay in amplitude was accomplished by an interrupted feedback arrangement. Although there are some critical differences, this decay free MME soliton generation is similar to the situation in optics in which a soliton train can be maintained in a recirculating fiber optic loop with a rare earth doped fiber optic amplifier [12].

The critical elements for a decay free MME soliton pulse train are (1) feedback to boost the signal back to its original level on successive passes and thereby compensate for the decay in pulse amplitude during propagation in the YIG film and (2) a switch to interrupt the feedback before the high gain needed for a decay free train pushes the system into oscillation. Figure 1 shows the soliton pulse train generator setup, with the YIG film structure, a variable attenuator, and a microwave amplifier in a feedback loop. The feedback is interrupted by switch 1. Input pulses are

applied to the loop through the microwave source, the pulse generator, directional coupler DC-1, and switch 2. The input and output signals are monitored through directional couplers DC-2 and DC-3.

The initial input pulse circulates in the loop and produces a series of output pulses. The gain G in the loop is controlled by the attenuator and determines the decay or gain properties of the output pulse sequence. For $G < 1$, one has attenuation. For $G \geq 1$, one has a train of pulses of constant or increasing amplitude, provided that one can avoid oscillation. Oscillation is suppressed through the opening of switch 1 after every $40 \mu\text{s}$ or so for several microseconds.

The diagram in Fig. 2 shows the pulse timing and the role of the gain G in controlling the output pulse train response. During the times indicated by the long pulses labeled 1 ON in Fig. 2(a), the feedback loop is complete and circulation can occur. The input pulse to the film structure is shown by the signals labeled 2 ON. This 2 ON signal is also the first pulse shown for each of the

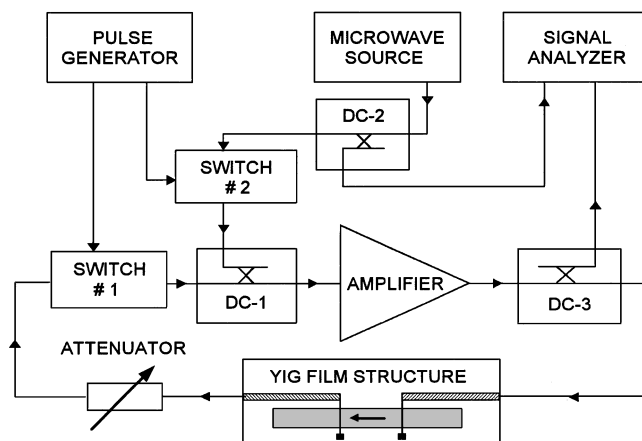


FIG. 1. Diagram of YIG film soliton pulse train generator interrupted feedback arrangement.

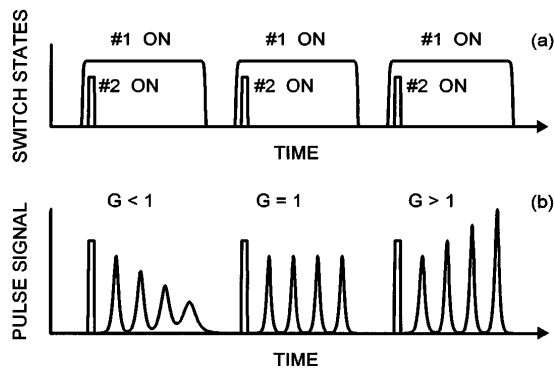


FIG. 2. Schematic illustration of (a) the switch timing pulses for the feedback control switch 1 and the input pulse control switch 2 and (b) output pulse sequences for three different limiting cases for the total feedback gain G , as indicated.

sequences in Fig. 2(b). These sequences show the nature of the output pulse trains picked up by coupler DC-3 in Fig. 1, for example, for three different gain situations.

The left side sequence in Fig. 2(b) is for a total loop gain G which is less than one. Here, the output pulse train generated by the recirculating signal decays in amplitude and broadens with each additional pass through the film structure. If the input power level is sufficient to produce a soliton, one or more of the initial pulse signals will correspond to solitons. With the continuing decay, however, the amplitude eventually falls below the threshold required for solitons and the pulses become dispersive and broad. The middle sequence of pulses shown in Fig. 2(b) is for the same input power, but the net gain is now equal to unity. Upon recirculation, the pulse enters the YIG structure at the same amplitude each time, and the condition for soliton propagation is preserved for each pass. The output sequence now corresponds to a train of soliton pulses all at the same amplitude. For the right side sequence of pulses, the net gain is now greater than unity. Under these conditions, one would expect the output pulse train to grow in amplitude as shown. This does not occur in practice because of soliton self-limiting. Data on this effect will be shown shortly.

The experiments used a $5.2 \mu\text{m}$ thick single crystal YIG film with a narrow linewidth and unpinned surface spins. The propagation structure consisted of a long and narrow 45 mm by 2 mm YIG film strip placed across two $50 \mu\text{m}$ wide 2 mm long strip line antennas separated by a distance $L = 3.2$ mm. A static magnetic field H of 1096 Oe was applied parallel to the long edge of the YIG strip and the propagation path from the input antenna to the output antenna. This configuration corresponds to the propagation of magnetostatic backward volume wave (MSBVW) pulses [13]. The MSBVW passband had a measured upper limit frequency of 5.046 GHz. The operating point carrier frequency for the experiments was set at $\omega_k/2\pi = 5.0$ GHz. The experiments used 25 ns rect-

angular pulses. The measured MME pulse group velocity was 2.42×10^6 cm/s.

For the above conditions, a YIG saturation induction $4\pi M_s = 1750$ G, and a gyromagnetic ratio γ defined by $|\gamma|/2\pi = 2.8$ GHz/kOe, an add-on static field increment of 32 Oe was needed to match the theoretical band edge to the measurement. A field of this order from magnetocrystalline anisotropy and strain is expected. With this adjustment, the theory gives a lowest order dispersion branch 5.0 GHz operating point wave number k of 120 rad/cm and a theoretical group velocity, $v_g = |\partial\omega_k/\partial k|$, of 2.43×10^6 cm/s. This velocity is in good agreement with the measured pulse velocity. This (ω_k, k) operating point was used for all of the soliton pulse train experiments described below.

As discussed in [8,10,11], and references therein, MME solitons may be formed in the MSBVW configuration at high power levels. This is because (1) the dispersion coefficient D , defined by $D = \partial\omega_k^2/\partial k^2$, is positive, and (2) the nonlinear response coefficient N , which relates the shift in ω_k as the amplitude of the signal is increased, is negative. When the Lighthill criterion, $DN < 0$, is satisfied, a compensation between the dispersion and the nonlinear frequency shift at high power can lead to stable soliton pulses. The 3.2 mm L value was long enough to produce bona fide soliton pulses and short enough to allow the soliton properties to be preserved over the entire propagation distance, in spite of the decay due to dissipation. Basic soliton propagation measurements as a function of input power and transducer separation distance similar to those described in [11] established the single soliton propagation regime for the structure.

Representative pulse train results are shown in Fig. 3. The four traces correspond to different values of the input power and the total loop gain. For traces 3(a), 3(b), and 3(c), the input power was 70.6 mW. For trace 3(d) the input power was 3.3 mW. Trace 3(a) is for a gain of -1.2 dB, or $G = 0.759$. Trace 3(b) is for a total gain of 0 dB or $G = 1$. Trace 3(c) is for a gain of $+0.6$ dB or $G = 1.148$. Trace 3(d) is for $+0.05$ dB or $G = 1.012$. Each trace shows a series of delayed output voltage pulses picked up from the recirculating signal. The first pulse in each sequence for 3(a), 3(b), and 3(c), at an amplitude close to 0.2 V, is just the amplified input pulse. For these traces, the power was such that the second pulse was always a soliton pulse. The input power for trace 3(d) was deliberately reduced below the soliton level. The time for one pass around the loop was 153 ns. This includes 21 ns of electronic delay and 132 ns for the MSBVW delay.

Trace 3(a) shows the pulse train which results when the input power is sufficient to produce a soliton for the first one or two recirculations but the total loop gain is less than unity. For the data shown, with $G = 0.786$, the feedback is not sufficient to maintain a soliton during more than a few initial recirculation cycles. These first few soliton pulses decay during the initial recirculation

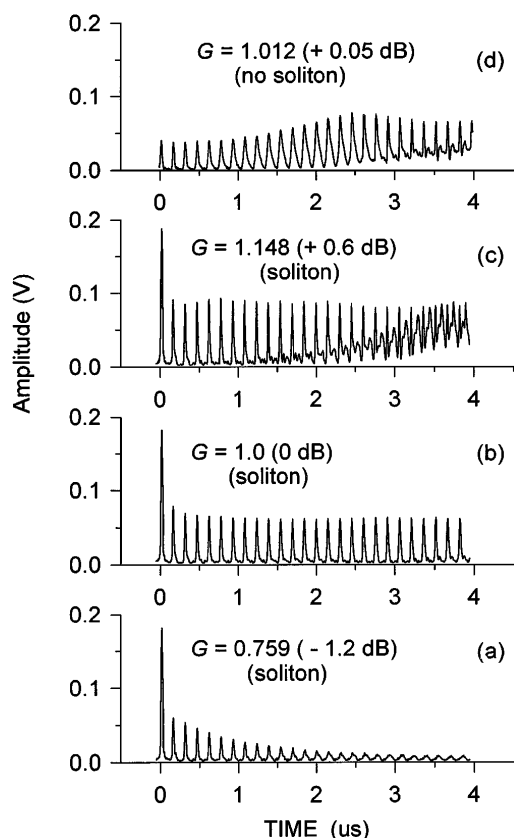


FIG. 3. Four sequences of soliton train pulses for different values of the loop gain, as indicated. The trains were produced from rectangular input pulses 25 ns in width applied to the coupler input DC-2 in Fig. 1. For (a), (b), and (c) the input power was held constant at 70.6 mW. For (d), the input power was reduced to 3.3 mW.

cycles. As the amplitude falls below the critical level needed to maintain soliton properties, the broadening and decay associated with dispersion come into play and the pulse train degrades to a series of broad, distorted, and low level pulses.

For trace 3(b), the input power was the same as for 3(a) but the total gain G was set to be unity. This trace shows a train of output pulses which stabilizes after three recirculations to yield pulses of fixed amplitude and width. The train is shown for cumulative times out to 4 μ s. The pulse width is maintained at about 19 ns, and the same train continues out to approximately 40 μ s. It is important to emphasize the extraordinary result represented by this trace. The fact that the pulse train continues undistorted for 250 recirculations attests to the soliton nature of the pulses. If the dispersion was not compensated by the nonlinear response, one would see significant broadening and decay during the extended recirculation. The observed 40 μ s lifetime for the soliton pulse train is about 2 orders of magnitude larger than the single soliton survival time found in [11].

For trace 3(c), the total loop gain has been increased a value greater than unity, $G = 1.148$. The input power

was the same as for traces 3(a) and 3(b). The sequence in trace 3(c) shows two important effects. First, it is noteworthy that, in spite of the higher gain, one does not see a pulse-to-pulse increase in amplitude of the sort shown schematically in the right side pulse sequence for $G > 1$ in Fig. 2(b). This is explained by the self limiting soliton response characteristic [8,10]. Once one exceeds the critical input level needed to produce a soliton at the output, any further increase in the input power results in a decrease in the peak output power as one moves into the regime of a multisoliton response [10]. When feedback is part of the process, this drop in output peak power leads to a self limiting effect.

The second important effect concerns the background output power level. Trace 3(c) shows the appearance of a parasitic background signal after about 1.5 μ s cumulative delay which increases to dominate the entire response characteristic after 4 μ s of cumulative delay. It is clear that when the gain exceeds unity, even by a small amount, the resultant parasitic oscillations destroy the soliton pulse train response characteristic early on in the pulse train lifetime. Such effects are present even for trace 3(b). This parasitic buildup is the reason for the total train lifetime limit of 40 μ s. This effect is an important consideration for further study.

Recall that trace 3(d) was obtained for a gain G of 1.01 and a very low input pulse power of 3.3 mW. This power was not large enough to produce a soliton output pulse after the first recirculation. The multiple effects here are quite distinct. For the first several recirculations, the pulses have almost constant amplitude. This is due to the balance between the feedback amplification and the pulse decay in the YIG film. As the recirculation continues, dispersion comes into play and produces an initial broadening. With this initial broadening, however, the dispersion effects are reduced and the small loop gain produces an increase in the pulse-to-pulse amplitude. This increase is evident for recirculations from 5 to 16 or so. With the increase in amplitude after 16 recirculations or so, the nonlinearity becomes important and a pulse narrowing becomes evident. At the same time, the parasitic oscillations begin to contribute to the total output signal and this leads to severe pulse distortion as well.

In order to verify conclusively the soliton character of the pulses shown in Fig. 3(b), for example, pulse phase profiles [14] as well as amplitude profiles were measured. Figure 4 shows some representative results from these measurements. The top graph shows an expanded amplitude profile for a typical pulse in the pulse train in trace 3(b). The bottom graph shows the corresponding phase profile. Note that the time scales are now shown in ns and indicate relative times only. The phase profiles represent the change in the carrier phase from that expected for a purely harmonic carrier signal. The abrupt 360° jumps represent instrumentation effects and have no physical significance. The important feature of note for the phase pro-

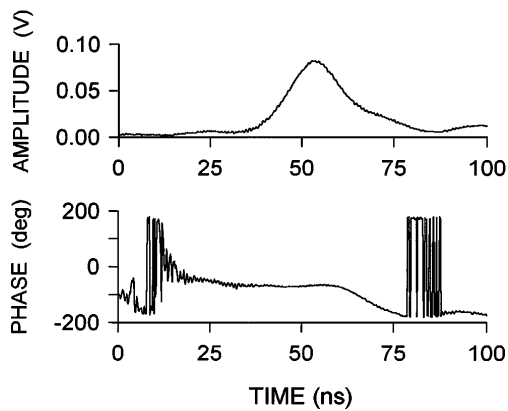


FIG. 4. Example data on soliton pulse train amplitude profiles from trace 3(b) along with companion measurements of the pulse phase profiles. The time scales shown are relative and do not track the time scale of trace 3(b).

file in Fig. 4 is the plateau of constant phase which occurs over the same time interval as the peak region for the amplitude profiles. As discussed in [14], this region of constant phase reflects the balance between the dispersion and the nonlinear response which produces the soliton. The observed region of constant phase, therefore, provides a clear demonstration of the soliton nature of the pulse train.

A second soliton test is also possible. From the nonlinear Schrödinger equation [11], one may obtain an analytical expression for the single soliton pulse width at half the peak amplitude,

$$\Gamma_t = \frac{2 \ln(2 + \sqrt{3})}{u_0 v_g} \left| \frac{D}{N} \right|^{1/2}, \quad (1)$$

where u_0 is the pulse amplitude and $N = \partial \omega_k / \partial |u|^2$ is the nonlinear response coefficient. The amplitude u_0 is related to the dynamic magnetization peak response \mathbf{m} through the condition $u_0 \approx |\mathbf{m}| / \sqrt{2} M_s$. Under the conditions given above, the theoretical D value is $648 \text{ cm}^2/\text{rad s}$. The N coefficient may be calculated under the assumption that the shift in ω_k with $|\mathbf{m}|$ is the same as the shift calculated from the linear theory with M_s replaced by $M_z = (M_s^2 - |\mathbf{m}|^2)^{1/2}$. In the limit $|u|^2 \rightarrow 0$, one obtains an operating point N -value of $-9.44 \times 10^9 \text{ rad/s}$.

The pulse amplitude in trace 3(b) is about 70 mV. Based on pulse transmission and reflection measurements as a function of transducer separation and without feedback, this level corresponds to a spin wave peak power of 1.2 mW and a u_0 value of 0.013, for an rms dynamic

magnetization response of about 1.8%. Equation (1) then yields a theoretical soliton half width of 22 ns, in good agreement with the measured width of 19 ns.

In conclusion, this Letter reports the first results on the generation of decay free magnetostatic wave envelope soliton trains in magnetic films. The trains have a time duration up to $40 \mu\text{s}$, 2 orders of magnitude larger than the single soliton lifetime. The phase profiles and widths of the individual pulses are as expected for bona fide MME solitons.

The work was supported in part by the U.S. Army Research Office, Grant No. DAAH04-95-1-0325, the National Science Foundation, Grant No. DMR-9400276, the Russian Foundation for Basic Research, Grant No. 96-02-19515, and the NATO Linkage Grant Program, Grant No. HTECH.LG 931489.

*Permanent address: St. Petersburg Electrotechnical University, 197376 St. Petersburg, Russia.

- [1] M.J. Ablowitz and H. Segur, *Solitons and the Inverse Scattering Transformation* (SIAM, Philadelphia, 1981).
- [2] G.L. Lamb, *Elements of Soliton Theory* (Wiley, New York, 1980).
- [3] R.K. Dodd, J.C. Eilbeck, J.D. Gibbon, and H.C. Morris, *Solitons and Nonlinear Wave Equations* (Academic, London, 1982).
- [4] G.P. Agrawal, *Nonlinear Fiber Optics* (Academic, Boston, 1995).
- [5] B.A. Kalinikos, N.G. Kovshikov, and A.N. Slavin, Zh. Eksp. Teor. Fiz. **94**, 159 (1988) [Sov. Phys. JETP **67**, 303 (1988)].
- [6] B.A. Kalinikos, N.G. Kovshikov, P.A. Kolodin, and A.N. Slavin, Solid State Commun. **74**, 989 (1990).
- [7] M. Chen, M.A. Tsankov, J.M. Nash, and C.E. Patton, Phys. Rev. Lett. **70**, 1707 (1993).
- [8] M. Chen, M.A. Tsankov, J.M. Nash, and C.E. Patton, Phys. Rev. B **49**, 12 773 (1994).
- [9] R. Marcelli and P. De Gasperis, IEEE Trans. Mag. **30**, 26 (1994).
- [10] J.M. Nash, C.E. Patton, and P. Kabos, Phys. Rev. B **51**, 15 079 (1995).
- [11] N.G. Kovshikov, B.A. Kalinikos, C.E. Patton, E.S. Wright, and J.M. Nash, Phys. Rev. B **54**, 15 210 (1996).
- [12] E. Desurvire, Phys. Today **47**, No. 1, 20 (1994).
- [13] R.W. Damon and J.R. Eshbach, J. Phys. Chem. Solids **19**, 308 (1961).
- [14] J.M. Nash, P. Kabos, and C.E. Patton, 1996 Digests of INTERMAG'96, IEEE Cat. No. 96CH35912, p. AE-03 (1996).